Caliphate Journal of Science & Technology (CaJoST)

ISSN: 2705-313X (**PRINT**); 2705-3121 (**ONLINE**) **Research Article**

Open Access Journal available at: https://cajost.com.ng/index.php/files and https://www.ajol.info/index.php/cajost/index

This work is licensed under a Creative Commons Attribution-NonCommercial 4.0 International License.

DOI: https://dx.doi.org/10.4314/cajost.v6i3.9

Article Info

Received: 28th May 2024

Revised: 27th October 2024

Accepted: 29th October 2024

[1]Department of Pure and Applied Physics, Veritas University Abuja, Nigeria
[2]Department of Physics, Bayero University Kano, Nigeria
[3]Department of Physics, Kano University of Science and Technology, Wudil, Kano, Nigeria

***Corresponding author's email:**

abengac@veritas.edu.ng

Cite this: *CaJoST*, 2024, 3, 323-332

Strong Absorption and The Double Folding Potential Using B3Y-Fetal Interaction

Raymond C. Abenga[1], Yahay Y. Ibrahim[2], Idriss D. Adamu[2] and Kassim L. Ibrahim[3]

This work examines the effects of strong absorption arising from nuclear potentials which are crucial to the understanding of the problem of nuclear interactions in other nonelastic channels. The double folding model was used to derive both the real and imaginary part of the nuclear optical potential using a mass-dependent B3Y-Fetal effective interaction constructed using the lowest order constrained variational (LOCV) approach. The absorption effect was incorporated in the calculations through the imaginary part of the optical potential. The folded potentials were found to be attractive and short-ranged over short internuclear distances of about $0 \leq r \leq 6\ fm$. The results of the plots of the S-matrix elements and those of the differential cross-sections of deuteron scattering from $^{24}_{12}\mathrm{Mg}$ were obtained. It was observed from the plots of the S-matrix elements that regions for which $|S_L| \sim 0$ existed between $0 \leq L \leq 5$ within the incident energies of $60 - 80\ \mathrm{MeV}$, implying strong absorption at these small impact parameters. Pronounced success was also achieved in the fit of the differential cross-sections of $\mathrm{d} + ^{24}_{12}\mathrm{Mg}$ within the energy range of 60 to $170\ \mathrm{MeV}$.

Keywords: B3Y-Fetal, Double-folding model, Elastic scattering, Folding potential, Strong absorption, S-matrix.

1. Introduction

The study of the most suitable form of nuclear potential to analyse nuclear interactions has received considerable attention in the field of nuclear physics in recent years [1]. Several theoretical models have been developed over the years to determine nuclear potentials to explain nucleon-nucleon interactions and as well as the structure of the interacting nuclei [2]. Unprecedented successes have been recorded in this regard by the use of computational tools in determining these nuclear optical potentials. To this effect, phenomenological potentials and folded potentials were derived and extensively used in nuclear structure and reaction studies [3]. These potentials derived in the elastic channel were expected to be used in other nonelastic channels.

Effects of strong absorption are ever present in the interaction of heavy ions and to account for this, one needs to construct the OP systematically [4]. To account for the strong absorption effect, the imaginary part of the optical potential was added using the double-folding model [5]. For strong absorption, we have that S_L vanishes: essentially, all the angular momenta L are removed from the elastic channel[6]. Due to the finite range of nuclear potentials and the diffuse edges of the nuclei, it is expected that a more realistic model would produce regions for which $S_L = 0$ but a smooth transition from 0 to 1 over a relatively small range of L [7].

In recent years, a good description of the nuclear optical potentials has been achieved by relating realistic nucleon-nucleon (NN) interaction and the densities of the interacting nuclei in the folding model (FM) framework [8]. The folding potentials are appealing since they can be used to predict the potentials of systems for which scattering data are not available. With the folded potentials, the ambiguities associated with the phenomenological potentials are eliminated [9]. The folded potentials are constructed by convoluting an effective nucleon-nucleon interaction with the density distribution of the incident particle and the target nucleus [10]. The potentials obtained through the folding models are found appropriate in the fact that they are simpler to handle. However, the folded potentials are used microscopically and the absorption effects are incorporated by taking the imaginary part phenomenologically. The success of the

 © 2024 Faculty of Science, Sokoto State University, Sokoto.

folding potentials in the description of the scattering data in the elastic channel has received considerable attention and recommendation over the years for its use in non-elastic channels [7, 11, 12]. In this work, the absorption effects are incorporated into the calculations by using the folding procedure to evaluate the imaginary part of the optical potential which is the main motivation of the present study.

This paper is organized as follows: In Section 2, a summary of the mass-dependent B3Y-Fetal effective interaction is given. In Section 3, we define the folding model of the present study. In Section 4, we present the results of our findings, and other relevant discussions are made. Finally, we make the conclusions of our findings in Section 5.

2. The B3Y-Fetal Effective Interaction

Different forms of nucleon-nucleon interactions such as the Michigan three Yukawa interaction (M3Y) interaction have been used for the studies of nuclear matter properties [13–16]. The M3Y interactions were used to study nuclear matter properties and reactions and were quite successful. In a recent study, mass-dependent interactions dubbed the B3Y-Fetal interaction derived using the lowest order constrained variational approach were constructed [17]. The interactions were derived using nuclei of mass numbers $A = 16$, 24, 40, and 90. Although the strengths of the interactions showed mass dependence, it was recommended that they could be used in the study of nuclear structure and reactions for all nuclei.

In this work, the isoscalar component of the central potential of the B3Y-Fetal interaction of Table VII from [17] was adopted. In its simple form, the isoscalar version of the B3Y-Fetal interaction is written as [18, 19],

$$V_D(r) = 7419.23\frac{e^{-4r}}{4r} - 1823.98\frac{e^{-2.5r}}{2.5r} \quad (1)$$

similarly, the exchange term is determined as:

$$V_{Ex}(r) = 4745.02\frac{e^{-4r}}{4r} - 1984.144\frac{e^{-2.5r}}{2.5r} - 7.8474\frac{e^{-0.7072r}}{0.7072r} \quad (2)$$

where $V_D(r)$ and $V_{Ex}(r)$ are the direct and exchange parts of the isoscalar component of the central potential of the B3Y-Fetal interaction.

This interaction is independent of the density of nuclear matter in which the interacting nucleons are embedded. It is, therefore, appropriate to consider the inclusion of the densities of the interacting systems. The inclusion of the density dependence to the bare nucleon-nucleon effective interaction is required for the nuclear matter to saturate rather than collapse [20]. The density dependence factor $f(\rho)$was added in the form prescribed by [21, 22],

$$V_{D(Ex)}(\rho, r) = f(\rho)V_{D(Ex)}(r) \quad (3)$$

The explicit form of the density dependence form factor under consideration is the exponential one and it is expressed as [23, 24],

$$f(\rho) = C\left(1 + \alpha\, exp\left(-\beta\rho\right)\right) \quad (4)$$

where C, α, and β are constants and ρ is the density of symmetric nuclear matter. The constant terms are determined by an iterative method in a manner to ensure saturation and to reproduce the correct value of the nuclear matter binding energy ($\epsilon = -16$ MeV) at $\rho = \rho_0 \approx 0.17\ \mathrm{fm}^{-3}$.

The exchange term of the effective interaction has been studied within the framework of the resonating-group method within a one-channel space [15]. It was found that the most important contributions of the exchange term come from single-nucleon exchange and core exchange. However, the latter is important only when the two nuclei have the same number of nucleons. In nucleon-nucleon scattering, this part is called knock-on exchange.

$$V_{pt} = V_{D(EX)}(1 - P_{EX}) \quad (5)$$

where $V_{D(EX)}$ are the direct and exchange parts of the effective interaction, P_{EX} is the operator that exchanges all the coordinates of the two nucleons by making the exchange part of the effective interaction local.

A direct consequence of equation (5) is that this makes the exchange term local, and hence it presents itself as another problem of localization. To delocalize the exchange term, two groups calculated it and concluded that it could be estimated quite accurately by adding zero-range pseudo-potential to the interaction V_{pt} in the form [25, 26],

$$V_{D(EX)}(1 - P_{EX}) \rightarrow V_D(r) + g(E)\hat{J}(E)\delta(r), \quad (6)$$

where $\hat{J}(E)\delta(r)$ is the zero-range pseudo-potential which accounts for the exchange part of the effective interaction [27] and $g(E)$ is the energy scaling factor. The zero-range pseudo-potential was evaluated as the Fourier transform of $V_{EX}(r)$ at the Fermi momentum k_0 of the incident nucleon to be ~ -361MeV [18, 28]. The energy scaling factor was approximated to that of the M3Y-Paris interaction to be $\left[1 - 0.005\left(\frac{E}{A}\right)\right]$ to account for the energy dependence of the effective interaction [24].

 © 2024 Faculty of Science, Sokoto State University, Sokoto.

3. METHOD: The Double Folding Model

The optical potential $U(r)$ of the present study was derived using the double-folding model. The double-folding model was used to obtain the optical potentials by convoluting an effective nucleon-nucleon interaction with the density distributions of the projectile and target nuclei [10]. Therefore, the folded potential $V_F(r)$ was obtained by averaging the DDB3Y-Fetal interaction over the density distributions of the interacting nuclei. In its simplest form, the DF potential is written as [15],

$$V_F(r) = \iint \rho_p(\boldsymbol{r}_p)\rho_t(\boldsymbol{r}_t)V_{pt}(\boldsymbol{r}_{tp})d\boldsymbol{r}_p d\boldsymbol{r}_t \quad (7)$$

where V_{pt} is the effective interaction (DDB3Y-Fetal), and $\rho_i(r_i)$ are the density distributions of the projectile and target nuclei $(i = p, t)$ and $\boldsymbol{r}_{tp} = r_t - r_p$. The geometry used in the description of the double-folding model is shown in Fig.1.

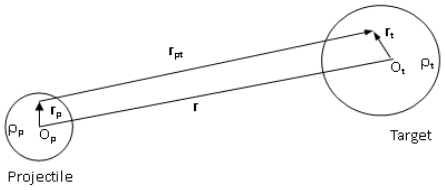

Fig. 1 Coordinates used in folding calculations.

The nuclear and charge densities of the projectile and the target nuclei were described using either the Fermi-type or the Gaussian-type function. In this study, the two-parameter Fermi (2pF) function was used. The 2pF function is defined as [29–31],

$$\rho_{n(p)}(r) = \rho_{0n(p)}\left[1 + \exp\left(\frac{r - R_{p(n)}}{a_{p(n)}}\right)\right]^{-1} \quad (8)$$

where ρ_0, $R_{p(n)}$, and $a_{p(n)}$ are the nuclear matter density parameters. The proton (neutron) half-density radii $R_{p(n)}$ were parameterised as[32],

$$\left.\begin{aligned} R_p &= 0.449 + 0.0071\left(\frac{Z}{N}\right) \\ R_n &= 0.446 + 0.0072\left(\frac{N}{Z}\right) \end{aligned}\right\} \quad (9)$$

where N and Z are the neutron and proton numbers of the projectile. The diffuseness parameters $a_{p(n)}$ were taken as the proton (neutron) surface thickness [31]. The value of ρ_0 was determined by the condition;

$$\rho_0 = \begin{cases} \int \rho_p(r)d^3r = Z \\ \int \rho_n(r)d^3r = A - Z \end{cases} \quad (10)$$

where A is the nucleus mass number of the projectile. The density distribution of the target nuclei was taken also to be of the 2pF function

$$\rho(r) = \rho_0\left[1 + \exp\left(\frac{r-c}{z}\right)\right]^{-1} \quad (11)$$

where c, and z are density parameters taken from [31].

The effective interaction included in equation (7) is real, and it is expected to account for the bare potential only. The immediate consequence was that the imaginary potential, which accounts for the polarization effect, must be constructed separately. However, this work accounted for the polarization effect by including an imaginary potential using the folding approach. With this proposition, the present nuclear potential was taken in the form [33]:

$$U(r) = (N_r + iN_i)V_F(r) + V_{Coul}(r) \quad (12)$$

where N_r and N_i are, respectively, the real and imaginary renormalization factors. The imaginary part of the potential was chosen to be the same as the real part but multiplied by a different renormalization factor. The renormalization factors were included to optimize the theoretical calculations and experimental data fit.

4. Results

The absorption effect of the folded potential was studied by constructing the optical potential of $\mathrm{d} + {}^{24}_{12}\mathrm{Mg}$ in the elastic channel within the incident laboratory energies of 60 to 170 MeV. The best-fit parameters of the folding calculations and other kinematical parameters of the calculations are listed in Table 1.

 © 2024 Faculty of Science, Sokoto State University, Sokoto.

Table 1: Best-fit parameters deduced from the double folding calculations and other kinematical parameters of elastic scattering of $d + {}^{24}_{12}Mg$.

Target	E_{lab}(MeV)	N_r	N_i	k (fm^{-1})	η	σ_r(mb)
${}^{24}Mg$	60.0	1.30	0.60	2.212	0.345	1048.35
	64.0	1.20	0.60	2.284	0.334	1021.51
	68.0	1.20	0.60	2.354	0.324	1005.45
	72.0	1.20	0.60	2.423	0.315	989.99
	76.0	1.20	0.65	2.456	0.307	995.74
	80.0	1.15	0.58	2.554	0.229	947.67
	90.0	1.18	0.6	2.709	0.282	925.06
	170.0	1.20	0.75	3.723	0.205	770.26

The absorption effect was accounted for by adding the imaginary part of the optical potential through the double-folding model. Both the real and imaginary potentials were taken the same but multiplied by different renormalization factors N_r and N_i respectively. In the folding calculations, larger renormalisation factors N_r were required for the real part of the optical potential while smaller ones N_i were deduced for the imaginary part of the optical potential. The calculated reaction σ_r cross-sections at corresponding incident energies are shown in Table 1. The values of σ_r in the present calculation are however found to be smaller than those calculated using phenomenological and semi-microscopic potentials [11, 34]. The large values of the σ_r is the manifestation of the absorption effect of the nuclear potential as included by the choice of the imaginary potential. However, it was observed that the values of σ_r decreased steadily as the incident energy was increased.

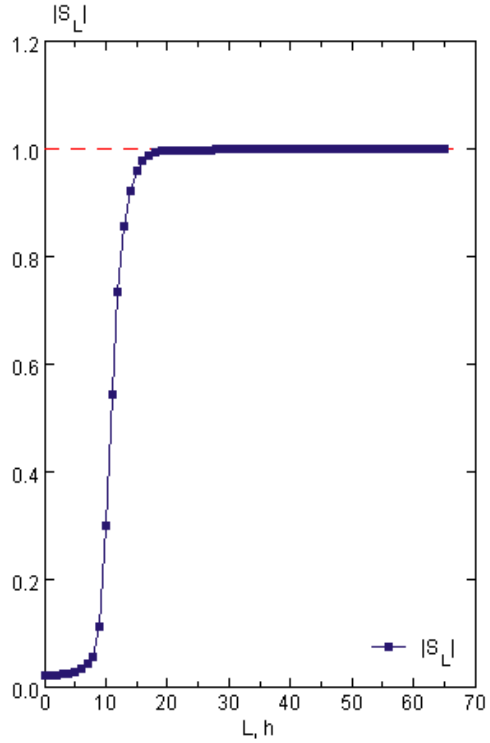

Fig. 2 Modulus of the elastic S-matrix of $d + {}^{24}_{12}Mg$ at $E_{lab} = 60$ MeV.

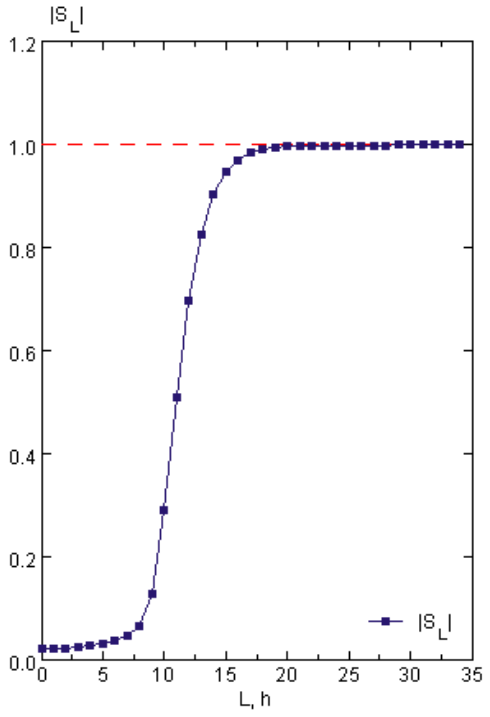

Fig. 3 Modulus of the elastic S-matrix of $d + {}^{24}_{12}Mg$ at $E_{lab} = 64$ MeV.

 © 2024 Faculty of Science, Sokoto State University, Sokoto.

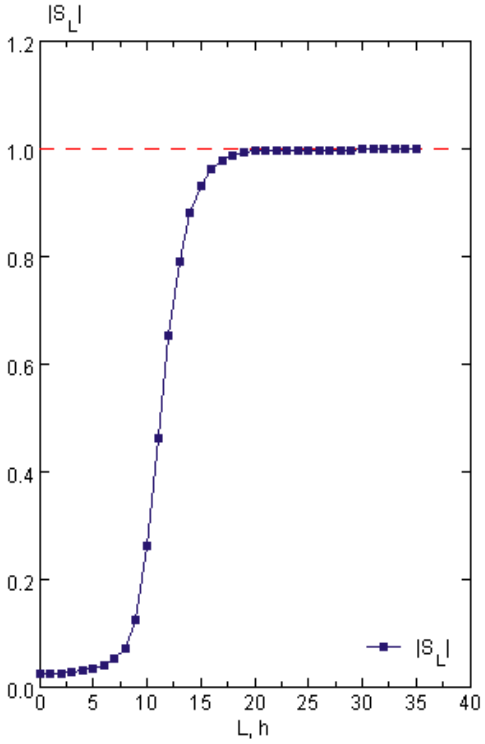

Fig. 4 Modulus of the elastic S-matrix of $d + {}^{24}_{12}Mg$ at $E_{lab} = 68$ MeV.

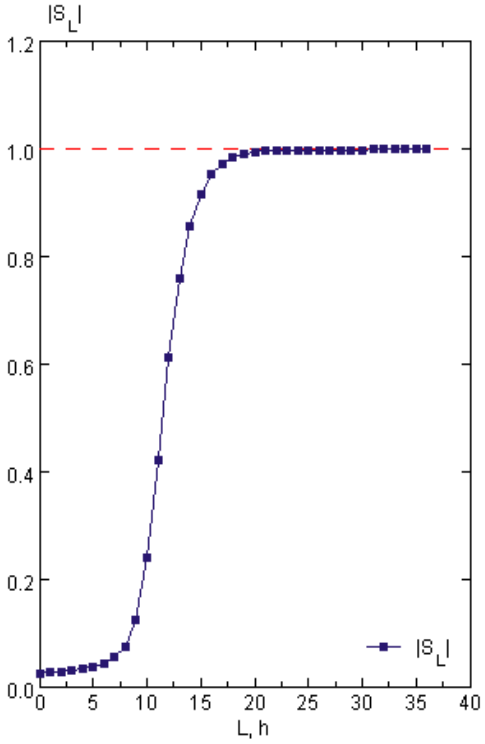

Fig. 5 Modulus of the elastic S-matrix of $d + {}^{24}_{12}Mg$ at $E_{lab} = 72$ MeV.

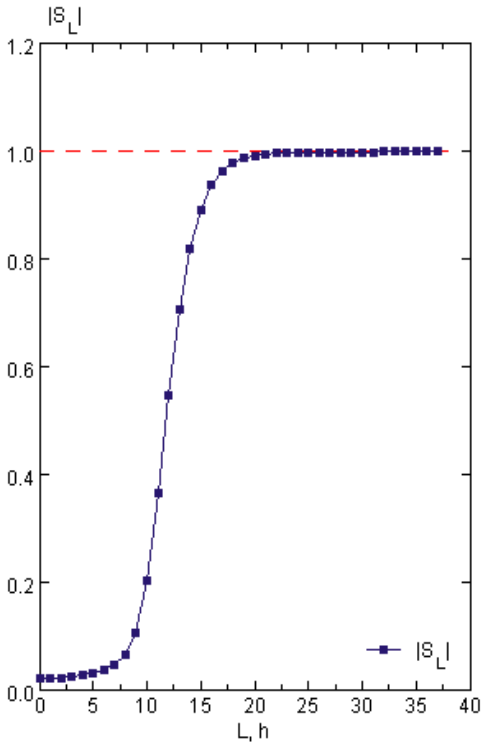

Fig. 6 Modulus of the elastic S-matrix of $d + {}^{24}_{12}Mg$ at $E_{lab} = 76$ MeV.

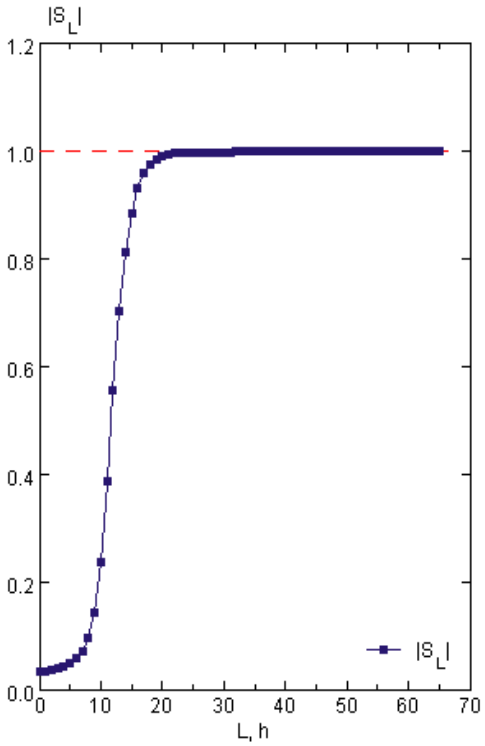

Fig. 7 Modulus of the elastic S-matrix of $d + {}^{24}_{12}Mg$ at $E_{lab} = 80$ MeV.

 © 2024 Faculty of Science, Sokoto State University, Sokoto.

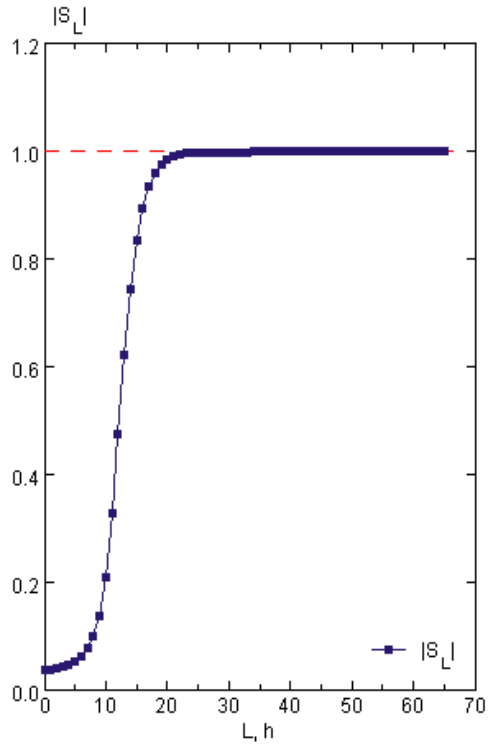

Fig. 8 Modulus of the elastic S-matrix of $d + {}^{24}_{12}Mg$ at $E_{lab} = 90$ MeV.

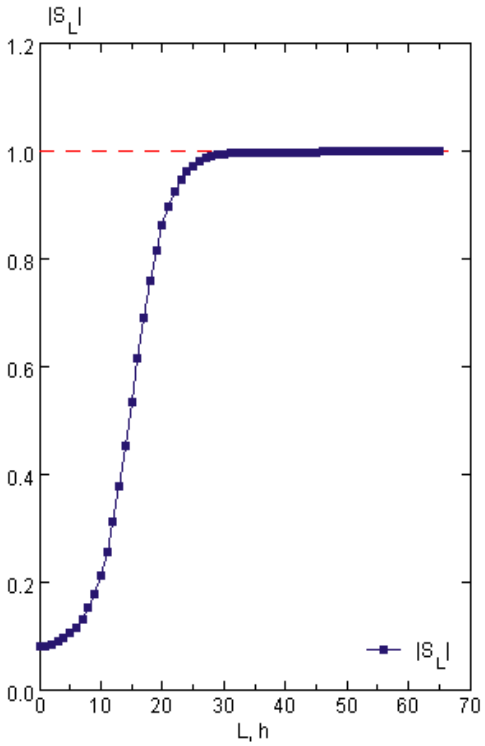

Fig. 9 Modulus of the elastic S-matrix of $d + {}^{24}_{12}Mg$ at $E_{lab} = 170$ MeV.

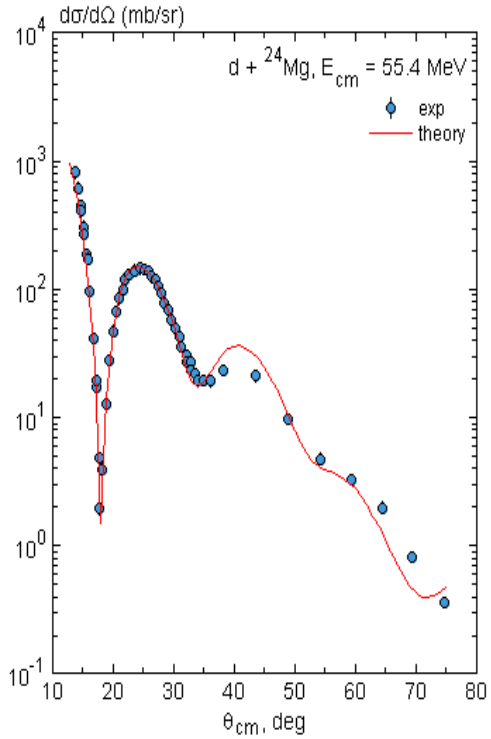

Fig. 10 Angular distribution of $d + {}^{24}_{12}Mg$ elastic scattering at $E_{lab} = 60$ MeV.

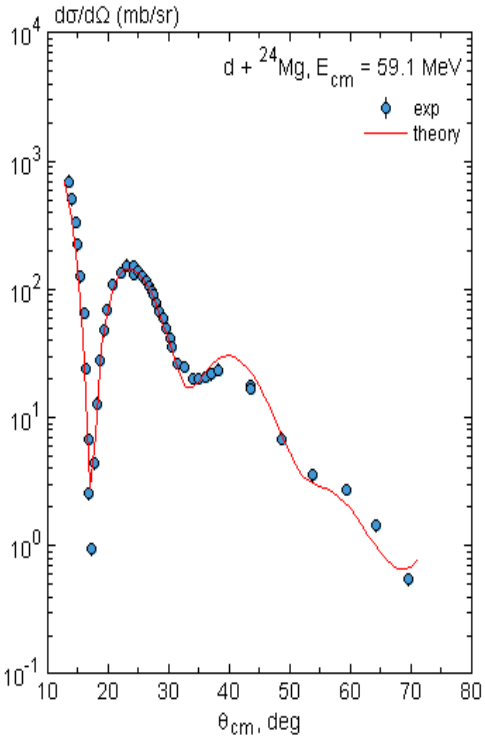

Fig. 11 Angular distribution of $d + {}^{24}_{12}Mg$ elastic scattering at $E_{lab} = 64$ MeV.

 © 2024 Faculty of Science, Sokoto State University, Sokoto.

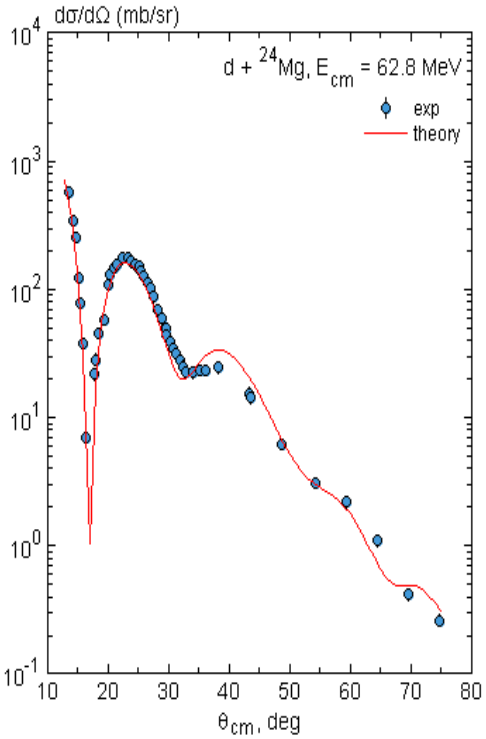

Fig. 12 Angular distribution of $d + {}^{24}_{12}Mg$ elastic scattering at $E_{lab} = 68$ MeV.

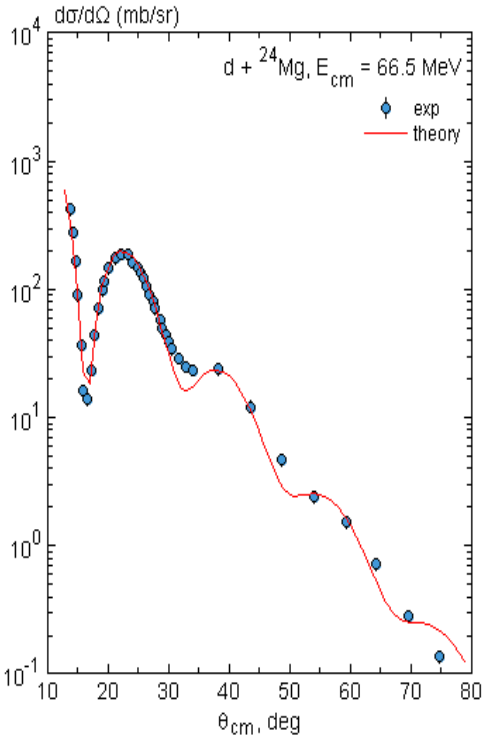

Fig. 13 Angular distribution of $d + {}^{24}_{12}Mg$ elastic scattering at $E_{lab} = 72$ MeV.

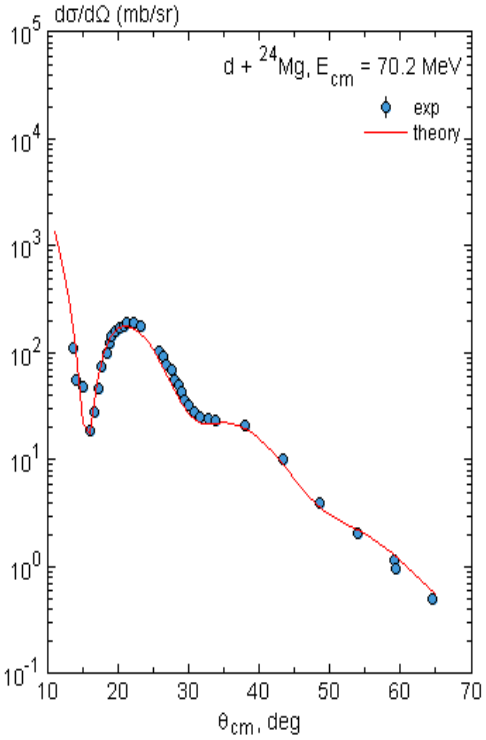

Fig. 14 Angular distribution of $d + {}^{24}_{12}Mg$ elastic scattering at $E_{lab} = 76$ MeV.

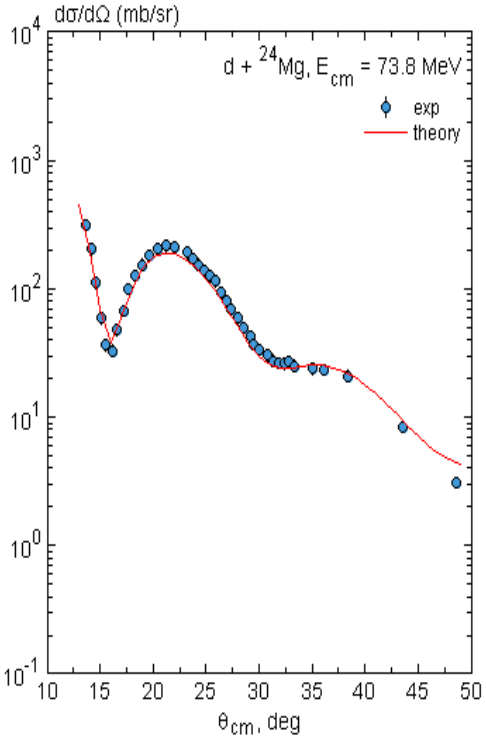

Fig. 15 Angular distribution of $d + {}^{24}_{12}Mg$ elastic scattering at $E_{lab} = 80$ MeV.

 © 2024 Faculty of Science, Sokoto State University, Sokoto.

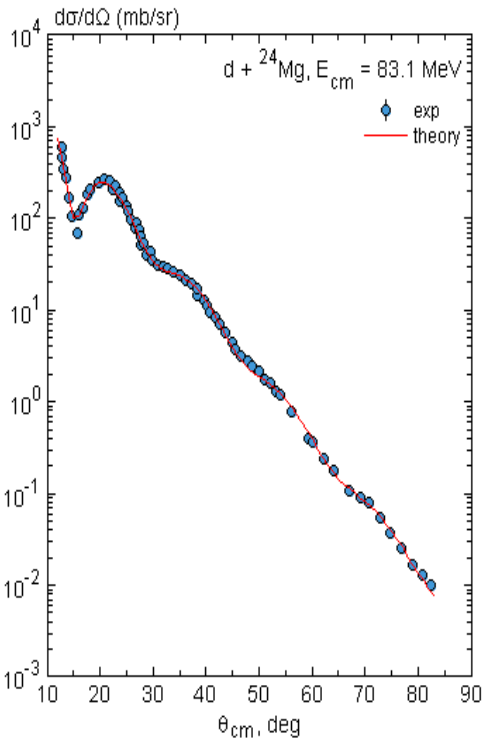

Fig. 16 Angular distribution of $d + {}^{24}_{12}Mg$ elastic scattering at $E_{lab} = 90$ MeV.

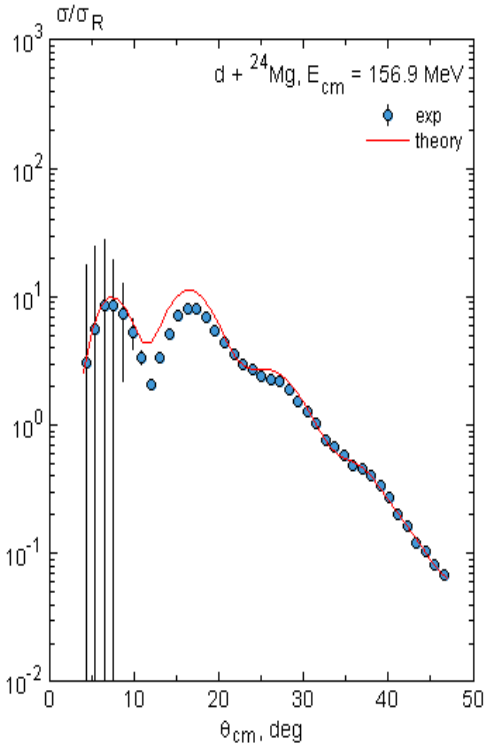

Fig. 17 Angular distribution of $d + {}^{24}_{12}Mg$ elastic scattering at $E_{lab} = 170$ MeV.

The moduli of the S-matrix were evaluated and the plots are shown in Figs. 2-9. In these figures, it was observed that the moduli obtained at all energies take ranges of values for which $|S_L| < 1$. Absorption effects were observed at all energies but were, however, seen to decrease with increasing energy. The decrease in the absorption effect as seen in these S-matrix plots is also evident as seen in the decreasing values of σ_r with increasing energy as shown in Table 1. Within the incident energies of 60 to80 MeV, regions for which $|S_L| \sim 0$ between $0 \leq L \leq 5$ implying strong absorption at these small impact parameters. At the incident energies 90 and 170 MeV, absorption effects were seen at small impact parameters but regions for which $|S_L| = 0$ were not observed.

The differential cross-sections were also calculated and fitted to corresponding experimental data to ascertain the suitability of the formulated optical potential using the B3Y-Fetal interaction. The results of the differential cross-sections of the present calculations are shown in Figs. 10-17. The observed diffraction patterns were well reproduced by the present calculations and reasonably good fits were obtained at all energies. The cross-sections were also seen to drop rapidly with increasing energy. This also confirms the impact of the formulated potential on the observed absorption effect. In general, satisfactory fits between the experimental data and the theoretical calculations were achieved using the B3Y-Fetal interaction in the folding model.

5. Conclusion

The effects of strong absorption were studied using the calculated folded potentials of $d + {}^{24}_{12}Mg$ in the elastic channel within the incident laboratory energies of 60 to 170 MeV. Sufficient evidences of strong absorption were observed as seen in the large values of the reaction cross-sections of Table 1 and the plots of the moduli of the S-matrix. The plots of the moduli of the elastic S-matrix elements as a function of total orbital angular momentum revealed that the real and imaginary parts of the optical potential contributed to the elastic scattering data. It was also observed that the nuclear part of the OP contributed to only a small range of *L* values. In these regions of small impact parameters, the effects of strong absorptions were observed, as $0 \leq |S_L| < 1$. Beyond the region of the small impact parameters, the nuclear potential vanished, and only the Coulomb potentials contributed to the elastic scattering data as $|S_L| = 1$. Furthermore, the calculated differential cross-sections are in good agreement with those obtained experimentally. The success of the present study should motivate the application of the current formulation and the B3Y-Fetal interaction to studies of nuclear reactions in other nonelastic channels.

Conflict of interest

The authors declare no conflict of interest.

 © 2024 Faculty of Science, Sokoto State University, Sokoto.

Acknowledgements

One of the authors (Raymond C. Abenga) wishes to thank Prof. Yahaya Y. Ibrahim for his sacrifices and determination to see to the completion of this work even when his health was threatened. This work is dedicated to Prof. Yahaya Y. Ibrahim.

References

[1] M. E. Kurkcuoglu, H. Aytekin, and I. Boztosun, "An Investigation of the $^{16}O + {}^{16}O$ Elastic Scattering by Using Alpha-Alpha Double Folding Potential in Optical Model Formalism," *Mod. Phys. Lett. A*, vol. 21, no. 29, pp. 2217–2232, 2006.

[2] A. A. Ibraheem, A. Branch, M. E. Farid, and E. F. Elshamy, "Comprehensive Examination of the Elastic Scattering Angular Distributions of $^{10}C + {}^{4}He$, ^{27}Al, ^{58}Ni, and ^{208}Pb Using Various Potentials," *Rev. Mex. Defisica*, vol. 69, no. June, pp. 1–13, 2023.

[3] H. A. Amer, A. Amar, S. Hamada, I. I. Bondouk, and F. A. El-Hussiny, "Optical and Double Folding Model Analysis for Alpha Particles Elastically Scattered from ^{9}Be and ^{11}B Nuclei at Different Energies," *World Acad. Sci. Eng. Technol. Open Sci. Index 110, Int. J. Chem. Mol. Eng.*, vol. 10, no. 2, pp. 161–166, 2016.

[4] M. E. Kurkcuoglu, H. Aytekin, and I. Boztosun, "Optical Model Analysis of the $^{16}O + {}^{16}O$ Nuclear Scattering Reaction around E_{Lab} = 5 MeV / Nucleon," *G. U. J. Sci.*, vol. 19, no. 2, pp. 105–112, 2006.

[5] F. Petrovich, R. J. Philpott, A. W. Carpenter, and J. A. Carr, "Spin Dependence in the Nucleus-Nucleus Optical Potential," *Nucl. Phys. A*, vol. 425, pp. 609–652, 1984.

[6] H. Matsuzaki, "Elastic and Inelastic Scatterings of Heavy Ions," *Prog. Theor. Phys.*, vol. 48, no. 5, pp. 1534–1546, 1972.

[7] G. R. Satchler, *Direct Nuclear Reactions*. Oxford University Press, 1983.

[8] M. E. Farid, Z. M. M. Mahmoud, and G. S. Hassan, "Analysis of Heavy Ions Elastic Scattering Using the Double Folding Cluster Model," *Nucl. Phys. A*, vol. 691, pp. 671–690, 2001.

[9] M. E. Farid, "Heavy Ion Double Folding Cluster Optical Potentials," *Phys. Rev. C*, vol. 65, no. June, pp. 11–13, 2002, doi: 10.1103/PhysRevC.65.067303.

[10] K. Hagino, T. Takehi, and N. Takigawa, "No-Recoil Approximation To The Knock-On Exchange Potential in the Double Folding Model for Heavy-Ion Collisions," *Phys. Rev. C - Nucl. Phys.*, vol. 74, no. 3, pp. 2–5, 2006, doi: 10.1103/PhysRevC.74.037601.

[11] M. E. Farid, L. Alsagheer, W. R. Alharbi, and A. A. Ibraheem, "Analysis of Deuteron Elastic Scattering in the Framework of the Double Folding Optical Potential Model," *Life Sci. J.*, vol. 11, no. 5, pp. 208–216, 2014, doi: http://dx.doi.org/110.21043/equilibrium.v3i2.1268.

[12] K. Behairy, M. M. Zakaria, and M. A. Hassanain, "Elastic and Inelastic α-Scatterings from ^{58}Ni, ^{116}Sn, and ^{208}Pb Targets at 288, 340, 480, and 699 MeV," *Brazilian J. Phys.*, vol. 54, no. 5, pp. 1–5, 2015, doi: 10.1007/s13538-015-0351-x.

[13] A. M. Kobos, B. A. Brown, P. E. Hodgson, G. R. Satchler, and A. Budzanowski, "Folding Model Analysis of α-Particle Elastic Scattering with a Semirealistic Density-Dependent Effective Interaction," *Nucl. Physics, Sect. A*, vol. 384, no. 1–2, pp. 65–87, 1982, doi: 10.1016/0375-9474(82)90305-0.

[14] N. Anantaraman, H. Toki, and G. F. Bertsch, "An Effective Interaction for Inelastic Scattering Derived from the Paris Potential," *Nucl. Physics, Sect. A*, vol. 398, no. 2, pp. 269–278, 1983, doi: 10.1016/0375-9474(83)90487-6.

[15] G. R. Satchler and W. G. Love, "Folding Model Potentials from Realistic Interactions for Heavy-Ion Scattering," *Phys. Reports (Review Sect. Phys. Lett.*, vol. 55, no. 3, pp. 183–254, 1979, doi: 10.1016/0370-1573(79)90081-4.

[16] N. Burtebayev, D. M. Janseitov, Zh. Kerimkulov, D. Alimov, M. Nassurlla, D. S. Valiolda, B. Mauyey, A. S. Demyanova, Sh. Hamada, and A. Aimaganbetov, "Elastic and inelastic scattering of deuterons from ^{13}C," *J. Phys. Conf. Ser.*, vol. 1555, pp. 1–7, 2020, doi: 10.1088/1742-6596/1555/1/012028.

[17] J. O. Fiase, K. R. S. Devan, and A. Hosaka, "Mass Dependence of M3Y-Type Interactions and the Effects of Tensor Correlations," *Phys. Rev. C - Nucl. Phys.*, vol. 66, no. 1, pp. 014004–10, 2002, doi: 10.1103/PhysRevC.66.014004.

[18] R. C. Abenga, J. O. Fiase, and G. J. Ibeh, "Optical Model Analysis of $\alpha + {}^{40}Ca$ at E_{Lab}= 104 and 141.7 MeV Using a Mass-Dependent M3Y-Type Effective Interaction," *Niger. Ann. Pure Appl. Sci.*, vol. 3, no. 2, pp. 252–260, 2020.

[19] R. C. Abenga and J. O. Fiase, "Elastic Scattering of $^{12}C + {}^{12}C$ and $^{16}O + {}^{16}O$ Using an Effective Mass Dependent M3Y-Type Interaction," *Int. J. Innov. Res. Adv. Stud.*, vol. 6, no. 2, pp. 57–61, 2019.

 © 2024 Faculty of Science, Sokoto State University, Sokoto.

[20] G.-L. Zang *et al.*, “Double Folding Model Calculation Applied to the Real Part of Interaction Potential,” *High Energy Phys. Nucl. Phys.*, vol. 13, no. 7, pp. 634–641, 2007, doi: 10.3321/j.issn.

[21] S. A. Moharram and A. O. El-Shal, “Spin Polarized Cold and Hot Dense Neutron Matter,” *Turk J. Phys.*, vol. 26, pp. 167–177, 2002.

[22] S. Hamada, I. Bondok, and M. Abdelmoatmed, “Double Folding Potential of Different Interaction Models for $^{16}O + {}^{12}C$ Elastic Scattering,” *Brazilian J. Phys.*, pp. 1–6, 2016, doi: 10.1007/s13538-016-0450-3.

[23] D. T. Khoa and W. Von Oertzen, “A nuclear Matter Study Using The Density-Dependent M3Y Interaction,” *Phys. Lett. B*, vol. 304, no. 12, pp. 8–16, 1993, doi: 10.1016/0370-2693(93)91391-Y.

[24] D. T. Khoa, W. Von Oertzen, and A. A. Ogloblin, “Study of the Equation of State for Asymmetric Nuclear Matter and Interaction Potential Between Neutron-Rich Nuclei Using the Density-Dependent M3Y Interaction,” *Nucl. Phys. A*, vol. 602, pp. 98–132, 1996, doi: 10.1016/0375-9474(96)00091-7.

[25] M. E. Brandan and G. R. Satchler, “The Interaction Between Light Heavy-Ions and What it Tells Us,” *Phys. Rep.*, vol. 285, pp. 143–243, 1997.

[26] W. G. Love and L. W. Owen, “Exchange Effects from Realistic Interactions in the Reformulated Optical Model,” *Nucl. Phys. A*, vol. 239, pp. 74–82, 1975, doi: 10.1016/0375-9474(75)91133-1.

[27] M. Modarres and M. Rahmat, “The LOCV Averaged Two-Nucleon Interactions Versus the Density-Dependent M3Y Potential for the Heavy-Ion Collisions,” *Nucl. Phys. A*, vol. 934, pp. 148–166, 2015, doi: 10.1016/j.nuclphysa.2014.11.006.

[28] R. C. Abenga, Y. I. Yahaya, and I. D. Adamu, “Double Folding Potential of Deuteron Elastic Scattering on Target Nuclei in the Mass Range of 50≤ A ≤ 208 Using a Mass-Dependent Effective Interaction,” *Bayero J. Phys. Math. Sci.*, vol. 01, no. 13, pp. 1–14, 2021.

[29] G. R. Satchler, “A Simple Effective Interaction for Peripheral Heavy-Ion Collisions at Intermediate Energies,” *Nucl. Phys. A*, vol. 579, pp. 241–255, 1994.

[30] A. L. El-Attar, M. E. Farid, and M. G. El-Aref, “Optical Model Analyses of Deuteron Inelastic Scattering,” in *9th International Conference for Nuclear Sciences and Applications, Sharm Al Sheikh (Egypt)*, Egypt, 2008, p. 1239.

[31] H. De Vries, C. W. De Jager, and C. De Vries, “Nuclear Charge-Density-Distribution Parameters from Elastic Electron Scattering,” *At. Data Nucl. Data Tables*, vol. 36, no. 3, pp. 495–536, 1987.

[32] S. D. Olorunfunmi and A. S. Olatinwo, “Analysis of Elastic Scattering Cross Sections of ^{16}O on ^{27}Al and ^{154}Sm Using the Semi-Microscopic Double Folding Model,” *Ife J. Sci.*, vol. 25, no. 2, pp. 239–250, 2023.

[33] R. C. Abenga, Y. Y. Ibrahim, and I. D. Adamu, “Double Folding Potential and the Deuteron-Nucleus Inelastic Scattering in the Optical Model Framework,” *Open Access Libr. J.*, vol. 10, pp. 1–16, 2023, doi: 10.4236/oalib.1109550.

[34] A. Kiss *et al.*, “The (D, D) and (D, D’) Scattering on ^{24}Mg at Energies Between 60 and 90 MeV,” *Nucl. Phys. A*, vol. 262, pp. 1–18, 1976.

 © 2024 Faculty of Science, Sokoto State University, Sokoto.